ACS APPLIED MATERIALS & INTERFACES

Letter

www.acsami.org

Characterizing Ion Profiles in Dynamic Junction Light-Emitting Electrochemical Cells

Tyko D. Shoji,[†] Zihua Zhu,[‡] and Janelle M. Leger*,[†]

[†]Department of Physics and Astronomy, Western Washington University, Bellingham, Washington 98225-9164, United States

[‡]Environmental Molecular Sciences Laboratory, Pacific Northwest National Laboratory, Richland, Washington 99352, United States

ABSTRACT: Organic semiconductors have the unique ability to conduct both ionic and electronic charge carriers in thin films, an emerging advantage in applications such as light-emitting devices, transistors, and electrochromic devices, among others. Evidence suggests that the profiles of ions and electrochemical doping in the polymer film during operation significantly impact the performance and stability of the device. However, few studies have directly characterized ion profiles within LECs. Here, we present an in-depth study of the profiles of ion distributions in LECs following application of voltage, via time-of-flight secondary ion mass spectrometry. Ion distributions were characterized with regard to film thickness, salt concentration, applied voltage, and relaxation over time. Results provide insight into the correlation between ion profiles and device performance, as well as potential approaches to tuning the electrochemical doping processes in LECs.

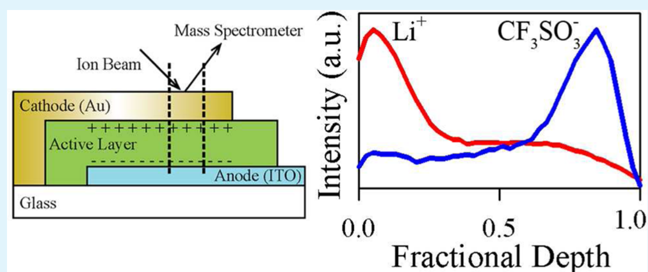

KEYWORDS: *polymer light-emitting electrochemical cell (LEC), organic electronics, electrochemical doping, conjugated polymers, secondary ion mass spectrometry*

INTRODUCTION

Polymer light-emitting electrochemical cells (LECs) offer a promising technology for lighting applications. LECs take advantage of the ionic conductivity of semiconducting polymers to achieve reduced charge injection barriers and low turn-on voltages. These devices are typically constructed in a layered structure, with a polymer film blended with ions sandwiched between an ITO bottom electrode and an evaporated top electrode. Ions within the polymer film dissociate under an applied bias and diffuse through the active layer. In the initially proposed model of LEC operation,[1,2] the electric field causes the cations and anions to accumulate along the cathode and anode, respectively (Figure 1). The ions act as counterions to maintain charge neutrality, thereby enabling electrochemical doping, leading to the formation of a p-doped region at the anode and an n-doped region at the cathode.[2−9] The doping process introduces mid-gap energy levels between the HOMO and LUMO energy levels, increasing the conductivity of the polymer and reducing charge injection barriers.[10,11] Light is emitted when electrons and holes meet and recombine in the thin intrinsic region between the doped regions.[7,8] Although the operational mechanism of LECs is in fact more complicated than this simple model would suggest,[5−9,12−16] it serves as an appropriate model of LEC operation for the purpose of this study.

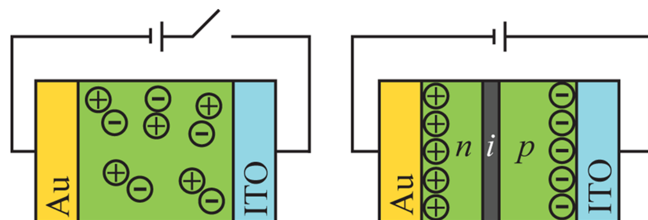

Figure 1. Schematic depicting p−i−n junction formation in an LEC with a gold cathode and ITO anode. The middle layer consists of a conducting polymer (green) and a dissolved salt (+/−).

Traditionally, inorganic salts such as lithium trifluoromethanesulfonate (lithium triflate, Li^+ $CF_3SO_3^-$) have been used as the ionic species in LECs. In these devices, the junction is dynamic; ions remain mobile in the film and the electrochemical doping process is also reversible. This impacts device performance in a number of ways. The junction does not persist without an external forward bias, as the ions relax over time, leading to turn-on times that are slow and depend on operational history. In addition, large applied voltages can result in heavy counterion build up at the electrodes, leading to overdoping and electrochemical side-reactions, and ultimately culminating in degradation of the active layer and shorter device lifetimes when operated at high brightness levels.[17] Attention has been paid to addressing these issues via the development of fixed-junction LEC technologies.[18−24] In fixed-junction devices, ions are immobilized within the film and the ion profile is maintained even after the bias is removed. This results in reduced turn-on times for subsequent bias

Received: September 4, 2013
Accepted: October 31, 2013
Published: October 31, 2013

 © 2013 American Chemical Society dx.doi.org/10.1021/am403805j | ACS Appl. Mater. Interfaces 2013, 5, 11509−11514

applications, and introduces the possibility of achieving a photovoltaic effect using an LEC structure.[24−29] Additionally, limiting the mobility of the ions after establishing the junction can prevent overdoping and electrochemical side reactions, and increased operational lifetimes have been demonstrated.[21]

It is clear that the advantages and challenges of LECs are closely associated with the ion profiles during and after device operation.[30−34] However, few studies have directly characterized ion movement and transport due to the inherent challenges in quantifying dynamic processes occurring at buried interfaces. A deeper understanding of ion mobility and distribution within LECs is essential for addressing device performance issues and maximizing performance. In previous work, Toshner et al.[34] used time-of-flight secondary ion mass spectrometry (ToF-SIMS) to obtain ion depth profiles for both fixed- and dynamic-junction LECs, correlating the junction fixation with ion immobilization and performing basic characterization of ion profiles in devices as a function of applied voltage. Here, we advance this work by using ToF-SIMS to examine ion depth profile dependence on film thickness, salt concentration, charging duration, and relaxation over time. Our measurements offer insight into the role of ionic species in the operation of dynamic-junction LECs.

■ EXPERIMENTAL SECTION

LECs were prepared at Western Washington University prior to ToF-SIMS measurements at the Environmental Molecular Sciences Laboratory (EMSL) at Pacific Northwest National Laboratory. For LEC fabrication, lithium triflate and trimethylolpropane ethoxylate were combined with Merck Livilux SPB-02T polymer in a mass ratio of 0.025:0.075:1, unless stated otherwise, and dissolved in chlorobenzene as described by Tang and Edman.[33] Lithium triflate was purchased from Aldrich and used as received. To examine the influence of salt concentration on ion distribution, we fabricated LECs with lithium triflate to polymer mass ratios between 0.025:1 and 0.150:1. For all devices, polymer and salt blends were mixed for several hours and spin-cast onto ITO-coated glass substrates with films thicknesses ranging from 100 to 200 nm. Atomic force microscopy was used to measure the thicknesses of the films. Gold contacts were deposited onto the active layer of the device to a thickness of 40 nm through thermal evaporation. Devices were stored and transported in an inert environment prior to testing at EMSL.

ToF-SIMS depth profiling was operated in a dual beam mode. A pulsing Bi^+ beam was used as the analysis beam. An O_2^+ sputtering beam was used for positive ion depth profiling and a Cs^+ sputtering beam was used for negative ion depth profiling. Prior to ToF-SIMS measurement, voltages were applied across the LECs for 3 min under an inert atmosphere, unless stated otherwise. Applying a bias across a device is referred to in this paper as 'charging,' with the gold contact serving as the cathode and the ITO serving as the anode under forward bias. The time required for sample loading and instrument preparation resulted in a minimum delay of approximately 1.5 to 2 h between device charging and ion depth profiling.

ToF-SIMS depth profiling measures ion counts with respect to measurement time. However, measurement time varies due to differences in device thickness. Here, ion profiles are presented instead with respect to fractional depth in the polymer film, with 0 corresponding to the cathode-polymer interface and 1 corresponding to the polymer-anode interface.

For each measurement, the polymer layer was identified by high counts of carbon signals (e.g., $C^{+/-}$) and low counts of both Au signals (e.g., $Au^{+/-}/Au_3^{+/-}$, from Au contact) and In signals (e.g. InO^-/In^+, from ITO substrate). During depth profile measurements, cation and anion markers were determined by selecting ions containing elements unique to each species. The Li^+ cations were directly measured while F^- ions served as a marker for the triflate anion.

■ RESULTS AND DISCUSSION

In the study conducted by Toshner et al.,[34] ToF-SIMS depth profiles of dynamic-junction LECs measured unexpected accumulations of Li^+ along the ITO anode in uncharged devices, an effect also observed in the present study (Figure 2c). A slight accumulation of F^- ions was also observed along

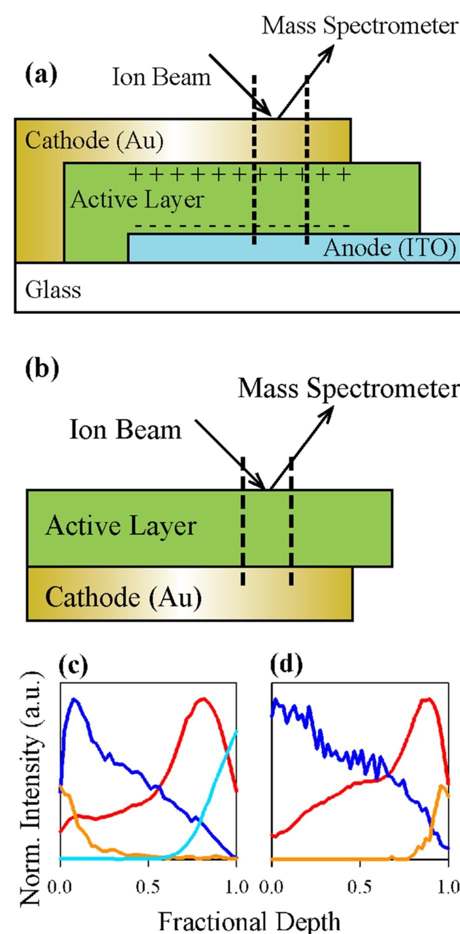

Figure 2. Schematics illustrating (a) a standard ToF-SIMS measurement and (b) an inverted depth profile measurement for a 100 nm thick active layer device. Profiles of Li^+ (red); F^- (dark blue); Au^-/Au^{3+} (orange); and In^+ (light blue) as obtained from a measurement of an uncharged dynamic-junction LEC measured (c) as shown in schematic a, and (d) as shown in schematic b.

the polymer−gold interface. It has been previously reported that in ToF-SIMS depth profiling, positive charges induced on the surface of a thin film by the sputtering ions produce large electric fields, resulting in ion migration within the film.[35] To determine if the initial observed nonuniform ion profiles had a similar origin, the polymer film and gold electrode of an uncharged LEC were carefully removed from the glass substrate and a ToF-SIMS depth profile measurement was conducted as

shown in Figure 2b. With this orientation, the depth profile instead revealed an accumulation of Li^+ ions at the polymer–gold interface (Figure 2d). Similarly, an accumulation of F^- ions was observed along the polymer–ITO interface. The locations of these increased ion concentrations remained consistent relative to the instrument, strongly suggesting that the ion beam is weakly attracting or repelling ions within the film and producing the anomalous peaks in the uncharged devices. Although these beam interactions result in the redistribution of ions near the boundaries of the polymer layer, thereby affecting the measured depth profiles, the effect appears to be consistent between measurements, making the depth profiles suitable for side-by-side comparison between devices.

The relaxation dynamics of ion profiles in dynamic-junction LECs with film thicknesses of 100, 150, and 200 nm charged at a 5, 10, and 15 V were examined by conducting depth profiles of devices over a period of 24 h after bias removal (The 15 V data are shown in Figure 3). Measurements were normalized to

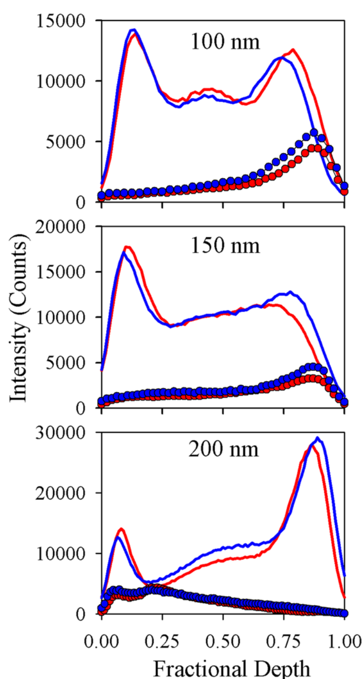

Figure 3. Li+ (2 h, solid red; 24 h, solid blue) and F^- (2 h, red circle; 24 h, blue circle) ion depth profiles for dynamic-junction LECs at 2 and 24 h after charging at 15 V. Devices were spin-cast to film thicknesses of 100, 150, and 200 nm.

fit either $^{113}In^+$ or $^{115}In^{16}O^-$ depth measurements to a standard profile to offset overall differences in intensities due to instrument fluctuations over time. This normalization factor was applied to Li^+ and F^- counts to enable direct comparison between measurements. Interestingly, no significant changes between the measurements taken from 2 to 24 h after charging were observed for any of the device thicknesses or charging voltages, in apparent contrast with our previous results that suggested relaxation back to the initial ion profile after about 12 h.[34] However, previous data analysis methods did not include corrections for instrument fluctuations, leading to misleading changes in ion profiles as a function of time of instrument operation. We believe that the analysis used in the current study makes the results presented here more accurate and reproducible. SKPM studies presented in the literature suggest that junctions within LECs rapidly relax immediately after the applied bias is removed.[8,9] It can be concluded that doping reversal, most likely accompanied by some amount of ion relaxation, occurs rapidly after bias removal. The present results, however, suggest that a significant amount of ion buildup along the electrodes may remain fixed long after bias removal even in dynamic-junction LECs, unless a reverse bias is applied. Interestingly, however, we have not observed that this persistent ion buildup results in any noticeable change in device turn-on time as a function of post-charging idle time.

The influence of charging duration on dynamic-junction LECs was examined by applying a constant voltage across pixels for different periods of time (Figure 4). Devices were charged

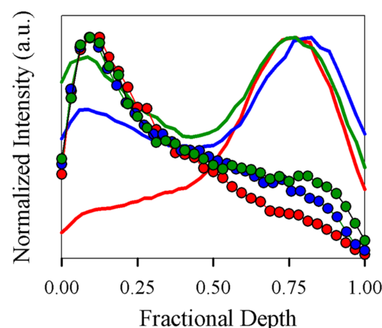

Figure 4. Li^+ and F^- ion depth profiles for dynamic-junction LECs with a 100 nm thick active layer charged at 7 V for 2 min (solid blue), 3 min (solid green), and uncharged (solid red) (Li^+), and 2 min (blue circle), 3 min (green circle), and uncharged (red circle) (F^-).

at 7 V for 2–3 min. Longer charge durations resulted in greater Li^+ ion concentrations along the cathode. F^- intensity also increased along the anode, to a lesser extent. The difference in the accumulation of cations and anions along the electrodes is most likely due to the size difference and, therefore, solid-state mobility between the Li^+ ion and the triflate anion. It is well-understood that in LECs, n-type doping is limited or delayed, observed beginning after the onset of p-type doping in planar devices, most likely due to side reactions that occur at the cathode rather than because of low mobility of the cations.[36] Consistent with this model, large concentrations of Li^+ along the cathode observed in the current study indicate that the presence of counterions is not a limiting factor in n-type doping.

The influence of charging voltage on the ion profiles established in LECs was studied by Toshner et al.[34] and is revisited here as a function of active layer thickness (Figure 5). As observed previously, Li^+ cation buildup increased along the cathode with increasing voltage. Similarly, the F^- ion marker profiles indicate increasing triflate anion buildup along the anode with higher voltages. However, the magnitude of this effect varies in devices of different film thicknesses. At all charging voltages, the buildup of Li^+ along the cathode and F^- along the anode relative to the rest of the film was found to be higher in LECs with thinner active layers (Figure 5a–c). At 15 V, the peak Li^+ concentration in the 100 nm thick film was approximately four times greater than the Li^+ concentration throughout the rest of the film (Figure 5a). In contrast, at 15 V, LECs with a 150 nm thick active layer demonstrated Li^+ buildup at the cathode that was approximately only twice as large as observed in other regions of the film (Figure 5d), while

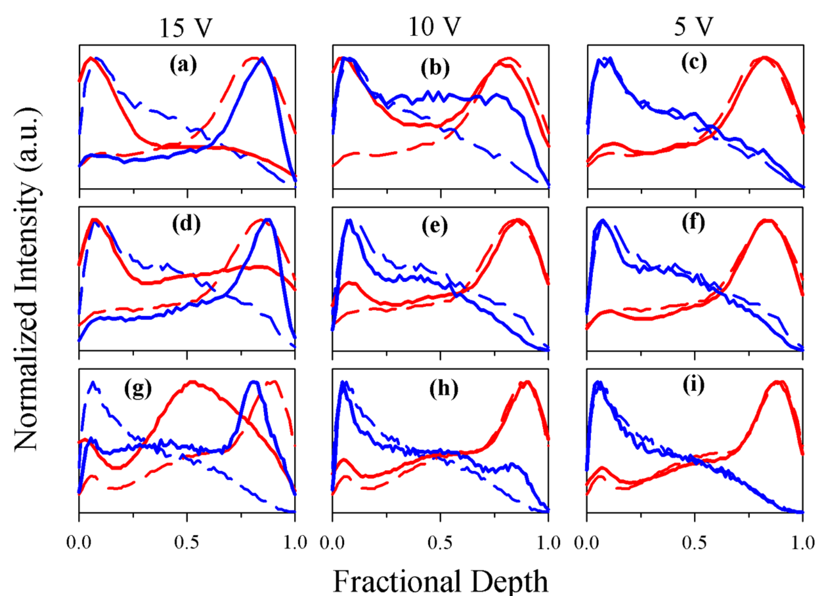

Figure 5. Normalized ion depth profiles for charged (Li^+, solid red; F^-, solid blue) and uncharged (Li^+, red dashed; F^-, blue dashed) lithium triflate LECs with film thicknesses of (a−c) 100, (d−f) 150, and (g−i) 200 nm charged at (c, f, i) 5, (b, e, h) 10, and (a, d, g) 15 V.

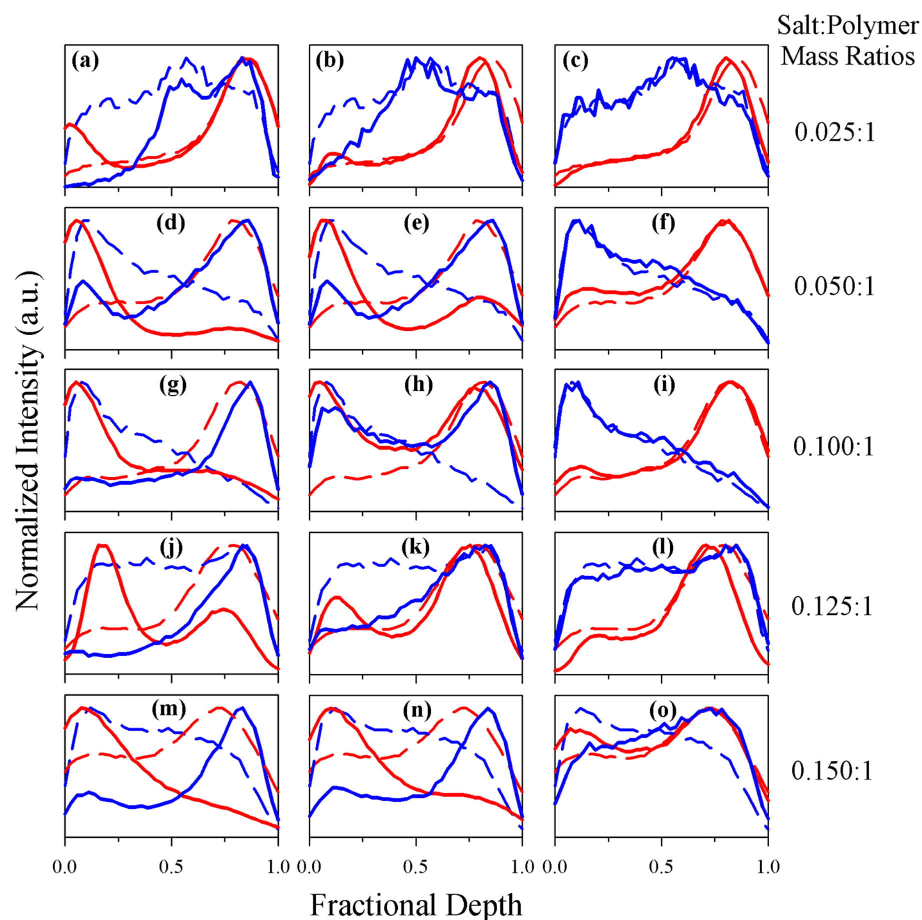

Figure 6. Normalized ion depth profiles for charged (Li^+, solid red; F^-, solid blue) and uncharged ($Li7^+$, red dashed; F^-, blue dashed) dynamic-junction lithium triflate LECs with lithium triflate:polymer mass ratios of (a−c) 0.025:1, (d−f) 0.05:1, (g−i) 0.1:1, (j−l) 0.125:1, and (m−o) 0.15:1 charged at (c, f, i, l, o) 5, (b, e, h, k, n) 10, and (a, d, g, j, m) 15 V.

a large amount of Li^+ remains in the center of the 200 nm thick film LECs or relaxes across the film immediately after bias removal (Figure 5g). Similar trends were observed for the triflate anion, although at higher voltages the differences among devices of different active layer thicknesses were less drastic. In general, the depth profiles demonstrate greater accumulations of cations and anions in thin active layers along the respective electrodes than in thick active layers. This is expected, as the

magnitude of the electric field within the active layer will be greater in thinner films. Consequently, ion migration and buildup along the electrodes is enhanced in thin films. Additionally, the widths of the ion concentration peaks as measured in terms of fractional depth of the active layer were similar between devices of different film thicknesses, implying that the thickness of p-doped and n-doped regions (or anion and cation buildup) scale with the thickness of the device.

Ion profiles in dynamic LECs were also investigated as a function of salt concentration in the active layer (Figure 6). With high salt concentrations, ions accumulate along the electrodes even with low applied bias (Figure 6o). High salt concentration LECs also appear to have wider ion distributions, possibly resulting in larger doped regions, and therefore a smaller intrinsic region. This supports previous studies examining salt concentration in LECs.[37] Generally, a high salt concentration facilitates doping throughout a greater region of the film, leading to a narrow intrinsic region and improved electroluminescence. In devices with low salt concentrations, regions of cation and anion depletion were observed relatively close to the cathode (Figure 6a, b), in agreement with other studies that have observed preferential p-doping and an intrinsic region near the cathode.[8,9,36] With higher salt concentrations, ion depletion was observed closer to the center of the film (Figure 6g, j, m), indicating the possibility of a shift in the position of the intrinsic region and/or incomplete depletion of ions from the intrinsic region. The latter has important implications for long-term device stability and is consistent with previously published results correlating device lifetime with salt concentration.[17,38]

CONCLUSIONS

We have measured the distribution of ions in dynamic-junction LECs using ToF-SIMS. The influence of beam interaction was explored, and the limits of this technique for quantitative analysis were determined. Ion buildup along the electrodes was observed two hours after device charging, and persisted for at least 24 h, suggesting that even in dynamic-junction LECs, ions may not completely redistribute to the intrinsic state after bias removal. Both charging voltage and charging duration appear to significantly influence the persistent ion buildup along the electrodes, with larger applied voltages and longer charging durations corresponding to greater ion accumulations.

The thickness of the active layer was observed to impact the relative amount of ion buildup at all tested voltages. Substantial ion accumulation along the electrodes occurred even at low voltages for LECs with thin active layers. The ratio between the salt and polymer was also found to alter the ion distribution, with wider cation distribution peaks in devices with high salt concentrations and higher relative concentration along the electrodes in the limits of low and high salt concentration ratios. Salt concentration in LECs also appeared to influence the location of the depleted ion region, with lower salt concentrations corresponding to depleted regions shifted toward the cathode, suggesting that the emission zone may also shift toward the cathode, in agreement with previous studies. With a deeper understanding of ion distributions, progress can be made toward improved lifetimes and performances in LECs.

AUTHOR INFORMATION

Corresponding Author

*E-mail: janelle.leger@wwu.edu.

Author Contributions

The manuscript was written through contributions of all authors. All authors have given approval to the final version of the manuscript.

Notes

The authors declare no competing financial interest.

ACKNOWLEDGMENTS

The authors gratefully acknowledge the National Science Foundation (DMR-1057209), the Washington NASA Space Grant Consortium Research Award, and Western Washington University for supporting this research. A portion of the research was performed using EMSL, a national scientific user facility sponsored by the Department of Energy's Office of Biological and Environmental Research and located at Pacific Northwest National Laboratory.

REFERENCES

(1) Pei, Q.; Yu, G.; Zhang, C.; Yang, Y.; Heeger, A. J. *Science* **1995**, *269*, 1086−1088.

(2) Pei, Q.; Yang, Y.; Yu, G.; Zhang, C.; Heeger, A. J. *J. Am. Chem. Soc.* **1996**, *118*, 3922−3929.

(3) Dick, D. J.; Heeger, A. J.; Yang, Y.; Pei, Q. *Adv. Mater.* **1996**, *8*, 985−987.

(4) Gao, J.; Heeger, A. J.; Campbell, I. H.; Smith, D. L. *Phys. Rev. B* **1999**, *59*, 2482−2485.

(5) Gao, J.; Dane, J. *Appl. Phys. Lett.* **2004**, *84*, 2778−2780.

(6) Gao, J.; Dane, J. *J. Appl. Phys.* **2005**, *98*, 063513−1-063513-8.

(7) Leger, J. M.; Carter, S. A.; Ruhstaller, B. *J. Appl. Phys.* **2005**, *98*, 124907−1-124907-7.

(8) Pingree, L. S. C.; Rodovsky, D. B.; Coffey, D. C.; Bartholomew, G. P.; Ginger, D. S. *J. Am. Chem. Soc.* **2007**, *129*, 15903−15910.

(9) Rodovsky, D. B.; Reid, O. G.; Pingree, L. S. C.; Ginger, D. S. *ACS Nano* **2010**, *4*, 2673−2680.

(10) Fesser, K.; Bishop, A. R.; Campbell, D. K. *Phys. Rev. B* **1983**, *27*, 4804−4825.

(11) Slinker, J. D.; DeFranco, J. A.; Jaquith, M. J.; Silveira, W. R.; Zhong, Y. W.; Moran-Mirabal, J. M.; Craighead, H. G.; Abruña, H. D.; Marohn, J. A.; Malliaras, G. G. *Nat. Mater.* **2007**, *6*, 894−899.

(12) deMello, J. C.; Tessler, N.; Graham, S. C.; Friend, R. H. *Phys. Rev. B* **1998**, *57*, 12951−12963.

(13) Holt, A. L.; Leger, J. M.; Carter, S. A. *J. Chem. Phys.* **2005**, *123*, 044704-1−044704-7.

(14) Matyba, P.; Maturova, K.; Kemerink, M.; Robinson, N. D.; Edman, L. *Nat. Mater.* **2009**, *8*, 672−676.

(15) van Reenen, S.; Matyba, P.; Dzwilewski, A.; Janssen, R. A. J.; Edman, L.; Kemerink, M. *J. Am. Chem. Soc.* **2010**, *132*, 13776−13781.

(16) Edman, L. In *Iontronics: Ionic Carriers in Organic Electronic Materials and Devices*; Leger, J. M., Berggren, M., Carter, S., Eds.; CRC Press: Boca Raton, FL, 2010; pp 101−118.

(17) Wågberg, T.; Hania, P. R.; Robinson, N. D.; Shin, J. H.; Matyba, P.; Edman, L. *Adv. Mater.* **2008**, *20*, 1744−1749.

(18) Yu, G.; Cao, Y.; Andersson, M.; Gao, J.; Heeger, A. J. *Adv. Mater.* **1998**, *10*, 385−388.

(19) Gao, J.; Li, Y.; Yu, G.; Heeger, A. J. *J. Appl. Phys.* **1999**, *86*, 4594−4599.

(20) Leger, J. M.; Rodovsky, D. B.; Bartholomew, G. P. *Adv. Mater.* **2006**, *18*, 3130−3134.

(21) Shao, Y.; Bazan, G. C.; Heeger, A. J. *Adv. Mater.* **2007**, *19*, 365−370.

(22) Kosilkin, I. V.; Martens, M. S.; Murphy, M. P.; Leger, J. M. *Chem. Mater.* **2010**, *22*, 4838−4840.

(23) Tang, S.; Irgum, K.; Edman, L. *Org. Electron.* **2010**, *11*, 1079−1087.

(24) Leger, J. M.; Bader, A. N. In *Iontronics: Ionic Carriers in Organic Electronic Materials and Devices*; Leger, J. M., Berggren, M., Carter, S., Eds.; CRC Press: Boca Raton, FL, 2010; pp 119−129.

(25) Gao, J.; Yu, G.; Heeger, A. J. *Appl. Phys. Lett.* **1997**, *71*, 1293–1295.
(26) Gao, J.; Yu, G.; Heeger, A. J. *Adv. Mater.* **1998**, *10*, 692–695.
(27) Cheng, C. H. W.; Lonergan, M. C. *J. Am. Chem. Soc.* **2004**, *126*, 10536–10537.
(28) Bernards, D. A.; Flores-Torres, S.; Abruña, H. D.; Malliaras, G. G. *Science* **2006**, *313*, 1416–1419.
(29) Leger, J. M.; Patel, D. G.; Rodovsky, D. B.; Bartholomew, G. P. *Adv. Funct. Mater.* **2008**, *18*, 1212–1219.
(30) Shin, J. H.; Xiao, S.; Edman, L. *Adv. Funct. Mater.* **2006**, *16*, 949–956.
(31) Shin, J. H.; Robinson, N. D.; Xiao, S.; Edman, L. *Adv. Funct. Mater.* **2007**, *17*, 1807–1813.
(32) Fang, J.; Matyba, P.; Robinson, N. D.; Edman, L. *J. Am. Chem. Soc.* **2008**, *130*, 4562–4568.
(33) Tang, S.; Edman, L. *J. Phys. Chem. Lett.* **2010**, *1*, 2727–2732.
(34) Toshner, S. B.; Zhu, Z.; Kosilkin, I. V.; Leger, J. M. *ACS Appl. Mater. Interfaces* **2012**, *4*, 1149–1153.
(35) Krivec, S.; Detzel, T.; Buchmayr, M.; Hutter, H. *Appl. Surf. Sci.* **2010**, *257*, 25–32.
(36) Fang, J.; Yang, Y.; Edman, L. *Appl. Phys. Lett.* **2008**, *93*, 063503–1-063503-3.
(37) van Reenen, S.; Matyba, P.; Dzwilewski, A.; Janssen, R. A. J.; Edman, L.; Kemerink, M. *Adv. Funct. Mater.* **2011**, *21*, 1795–1802.
(38) Fang, J.; Matyba, P.; Edman, L. *Adv. Funct. Mater.* **2009**, *19*, 2671–2676.